

**Frequent Derepression of the Mesenchymal Transcription Factor Gene *FOXC1* in Acute Myeloid Leukemia****Highlights**

- *FOXC1* is expressed in at least 20% of human AML in association with the HOXA/B locus
- *FOXC1* contributes to monocyte lineage differentiation block and clonogenic potential
- *FOXC1* collaborates with HOXA9 to accelerate onset of symptomatic leukemia
- Repression of *FOXC1* in normal stem and progenitor cells is PRC2 dependent

**Authors**

Tim D.D. Somerville, Daniel H. Wiseman, Gary J. Spencer, ..., Emma L. Williams, Edmund Cheesman, Tim C.P. Somerville

**Correspondence**

tim.somerville@cruk.manchester.ac.uk

**In Brief**

Somerville et al. report frequent derepression of *FOXC1* in human acute myeloid leukemia in association with the HOXA/B locus. *FOXC1* contributes to monocyte lineage differentiation block and enhanced clonogenic potential and collaborates with HOXA9 to accelerate leukemia onset in vivo.

**Accession Numbers**

GSE66256



# Frequent Derepression of the Mesenchymal Transcription Factor Gene *FOXC1* in Acute Myeloid Leukemia

Tim D.D. Somerville,<sup>1</sup> Daniel H. Wiseman,<sup>1</sup> Gary J. Spencer,<sup>1</sup> Xu Huang,<sup>1</sup> James T. Lynch,<sup>1</sup> Hui Sun Leong,<sup>2</sup> Emma L. Williams,<sup>1</sup> Edmund Cheesman,<sup>3</sup> and Tim C.P. Somerville<sup>1,\*</sup>

<sup>1</sup>Leukaemia Biology Laboratory

<sup>2</sup>Computational Biology Support Group

Cancer Research UK Manchester Institute, The University of Manchester, Manchester M20 4BX, UK

<sup>3</sup>Department of Diagnostic Paediatric Pathology, Royal Manchester Children's Hospital, Manchester M13 9WL, UK

\*Correspondence: [tim.somerville@cruk.manchester.ac.uk](mailto:tim.somerville@cruk.manchester.ac.uk)

<http://dx.doi.org/10.1016/j.ccell.2015.07.017>

## SUMMARY

Through *in silico* and other analyses, we identified *FOXC1* as expressed in at least 20% of human AML cases, but not in normal hematopoietic populations. *FOXC1* expression in AML was almost exclusively associated with expression of the *HOXA/B* locus. Functional experiments demonstrated that *FOXC1* contributes to a block in monocyte/macrophage differentiation and enhances clonogenic potential. *In vivo* analyses, *FOXC1* collaborates with *HOXA9* to accelerate significantly the onset of symptomatic leukemia. A *FOXC1*-repressed gene set identified in murine leukemia exhibited quantitative repression in human AML in accordance with *FOXC1* expression, and *FOXC1*<sup>high</sup> human AML cases exhibited reduced morphologic monocytic differentiation and inferior survival. Thus, *FOXC1* is frequently derepressed to functional effect in human AML.

## INTRODUCTION

Acute myeloid leukemia (AML) is a hierarchically organized, clonal neoplastic disorder sustained by a subpopulation of cells with long-term proliferative potential, often termed leukemia stem cells (LSCs) (Wiseman et al., 2014). In recent years there has been a concerted effort to understand the genetic, epigenetic, and transcriptional differences between AML cells and their normal cellular counterparts, with the longer term aim of developing therapeutic strategies that selectively target leukemia cells. One approach has been to prospectively isolate AML cells with immature progenitor immunophenotypes (immunophenotypic LSCs) and compare their transcriptional profiles with normal hematopoietic stem and progenitor cells (HSPCs) (Saito et al., 2010; Kikushige et al., 2010; Goardon et al., 2011). These studies have highlighted cell surface receptors CD25, CD32, and HAVCR2 (also known as TIM3) as candidate therapeutic targets in AML. These comparative data sets provide a

rich resource for further exploration of biological processes active in human AML. Of particular interest is the set of transcription factors expressed in AML, in view of their essential roles in regulation of gene expression and cell fate.

## RESULTS

### *FOXC1* Is Expressed in Human AML

To identify transcription regulators expressed in human AML HSPCs but not normal HSPCs, we analyzed levels of transcription factor genes (Vaquerizas et al., 2009) in three recent data sets (Saito et al., 2010; Kikushige et al., 2010; Goardon et al., 2011). Of those exhibiting significantly higher expression in AML HSPCs versus normal HSPCs, *FOXC1* was among the most highly upregulated in each study (Figures 1A–1C). Others similarly upregulated included *CEBPA*, *CEBPD*, *IKZF1*, and *IRF8*, known to be highly expressed in myeloid cells (Figures 1A–1C). High *FOXC1* expression (where probeset expression

### Significance

Our investigations highlight a frequent pathogenic mechanism in human AML: the tissue-inappropriate derepression of a mesenchymal forkhead box transcription factor gene with functional consequences and prognostic significance. They also highlight *FOXC1* as a *HOX*-collaborating factor. Continued *FOXC1* repression in normal hematopoietic cells is Polycomb repressive complex 2 (PRC2) dependent, because treatment of CD34<sup>+</sup> cells with distinct PRC2 inhibitors led to significant increases in its expression. However, bioinformatics analyses demonstrated that in AML, there is no widespread derepression of genes normally marked by Polycomb in CD34<sup>+</sup> cells. Thus *FOXC1* derepression in AML represents a locus-specific phenomenon rather than a genome-wide failure of Polycomb activity.

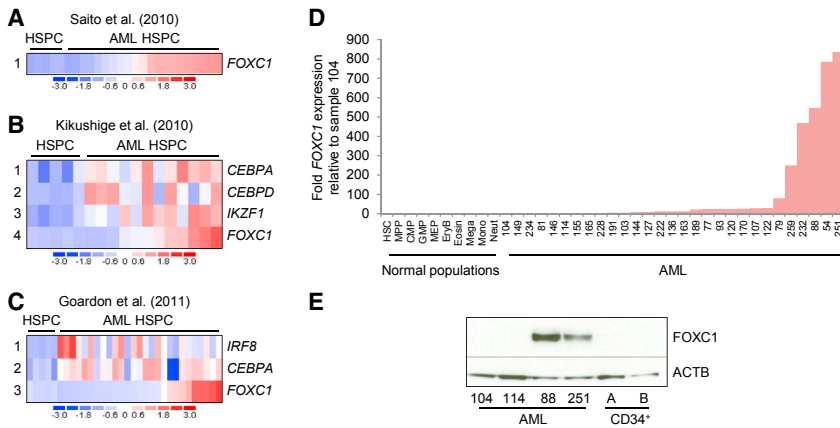


**Figure 1. Expression of *FOXC1* in Human AML**

(A–C) Heatmaps show the most highly upregulated transcription factor genes in the indicated studies. Transcription factor genes differentially expressed in AML HSPCs versus normal adult immunophenotypic BM HSPCs were identified using an unpaired t test (with  $p < 0.005$ ) and were ranked according to the mean fold change increase in expression (ranking number shown on the left of each heatmap row). Color scale indicates the standardized expression level for each gene. The definition of HSPCs in each study was (A)  $CD34^+CD38^-$  for both normal ( $n = 5$ ) and AML ( $n = 21$ ) cells; (B)  $CD34^+CD38^-Lin^-$  for normal cells ( $n = 5$ ) and  $CD34^+CD38^-$  for AML cells ( $n = 12$ ); and (C)  $CD34^+CD38^-CD90^+CD45RA^-Lin^-$  for normal cells ( $n = 5$ ) and

granulocyte-macrophage progenitor (GMP)-like ( $n = 21$ ), multipotent progenitor (MPP)-like ( $n = 3$ ), or  $CD34^+CD38^-CD90^+CD45RA^+$  ( $n = 3$ ) for AML samples.

(D) Bar chart shows relative expression of *FOXC1* in bulk primary human AML samples ( $n = 29$ ) and prospectively sorted normal human cell populations ( $n = 3$  separate individuals per cell type; Huang et al., 2014). See also Table S1. CMP, common myeloid progenitor; Eosin, eosinophils; EryB, erythroblast; HSC, hematopoietic stem cell ( $CD34^+38^-90^+45RA^-Lin^-$ ); Mega, megakaryocytes; MEP, megakaryocyte-erythrocyte progenitor; Mono, monocytes; Neut, neutrophils. AML sample numbers refer to the Biobank identifier.

(E) Western blot shows expression of *FOXC1* in the indicated AML and normal  $CD34^+$  cell samples.

See also Figure S1 and Tables S1–S3.

values for *FOXC1* were among the top 10% for protein-coding genes values) was observed in 48%, 50%, and 33% of samples analyzed in each study, respectively (Figures 1A–1C). Thus, *FOXC1* is among the most highly upregulated transcription factor genes in AML HSPCs.

*FOXC1* is a member of the forkhead box family of transcription factors, which are critical regulators of development and differentiation. In keeping with a requirement for *FOXC1* in mesenchymal differentiation, *Foxc1*-null mice die perinatally with skeletal, cardiac, and renal abnormalities, hydrocephalus, iris hypoplasia, and open eyelids (Kume et al., 1998). Humans with inherited haploinsufficiency of *FOXC1* due to mutation or deletion exhibit the Axenfeld-Rieger syndrome, characterized by similar features to the murine knockout (Nishimura et al., 1998; Kume et al., 1998). High *FOXC1* expression is associated with poor prognosis in breast and liver cancer (Ray et al., 2010; Xia et al., 2013), and its forced expression promotes an epithelial-to-mesenchymal transition and enhanced proliferation, migration, invasion, and drug resistance, through downstream mediators such as NF- $\kappa$ B and NEDD9 (Bloushtain-Qimron et al., 2008; Wang et al., 2012; Xia et al., 2013). Interestingly, *Foxc1* is highly expressed by *Cxcl12*-expressing adipo-osteogenic progenitors in mouse bone marrow (BM), and its deletion ablates hematopoietic stem cell (HSC) niches leading to reduced BM cellularity (Omatsu et al., 2014).

Deletion of *Foxc1* in normal murine BM does not affect hematopoiesis (Omatsu et al., 2014), suggesting redundancy or lack of expression. To determine whether *FOXC1* is expressed in normal human hematopoiesis, we performed quantitative PCR on flow-sorted populations of BM HSPCs and terminally differentiated cells, including neutrophils and monocytes (Figure 1D) (Huang et al., 2014). *FOXC1* expression was either absent or detected at very low level. In contrast, *FOXC1* transcripts were detected at a high level (greater than 200-fold increase over expression levels in the lowest expressing AML sample)

in 5 of 29 (17%) bulk AML blast samples tested (Figure 1D; Table S1) and at an intermediate level in 8 of 29 (28%) samples (20- to 200-fold increase over expression levels in the lowest expressing AML sample). Increased *FOXC1* transcripts in AML cells led to increased protein expression (Figure 1E), and *FOXC1* protein was not detected in normal human  $CD34^+$  cells (Figure 1E). These data demonstrate that the mesenchymal transcription factor *FOXC1* (which is neither expressed in nor required for normal hematopoiesis) is frequently highly expressed in human AML in both the stem/progenitor and bulk blast compartments.

### ***FOXC1* Expression in Human AML Is Associated with Mutations in *NPM1* and t(6;9)**

Our quantitative PCR analysis in bulk AML samples was confirmed by expression data from two recent studies. *FOXC1* was expressed at a high level (i.e., with a probeset expression value among the top 25% of protein-coding gene values) in 100 of 461 (22%) of presentation samples from a Dutch cohort of younger adults (aged <60 years) subsequently treated intensively (i.e., with anthracycline and cytarabine-based chemotherapy) on the Hemato-Oncologie voor Volwassenen Nederland (HOVON) protocols (Figure S1A) (Wouters et al., 2009). Similarly 36 of 163 (22%) samples selected to be representative of the genetic range of human AML also exhibited high expression (Figure S1B) (Cerami et al., 2012; Cancer Genome Atlas Research Network, 2013). High *FOXC1* expression was strongly associated with intermediate cytogenetic risk, normal karyotype, and the presence of an *NPM1* mutation or a t(6;9) translocation (Tables S2 and S3). High *FOXC1* expression was negatively associated with good cytogenetic risk, its associated karyotypes, and the presence of double *CEBPA* mutations (Table S2). In the Dutch study high *FOXC1* expression was strongly associated with the presence of FLT3 internal tandem duplications, but this was not seen in The Cancer Genome Atlas study

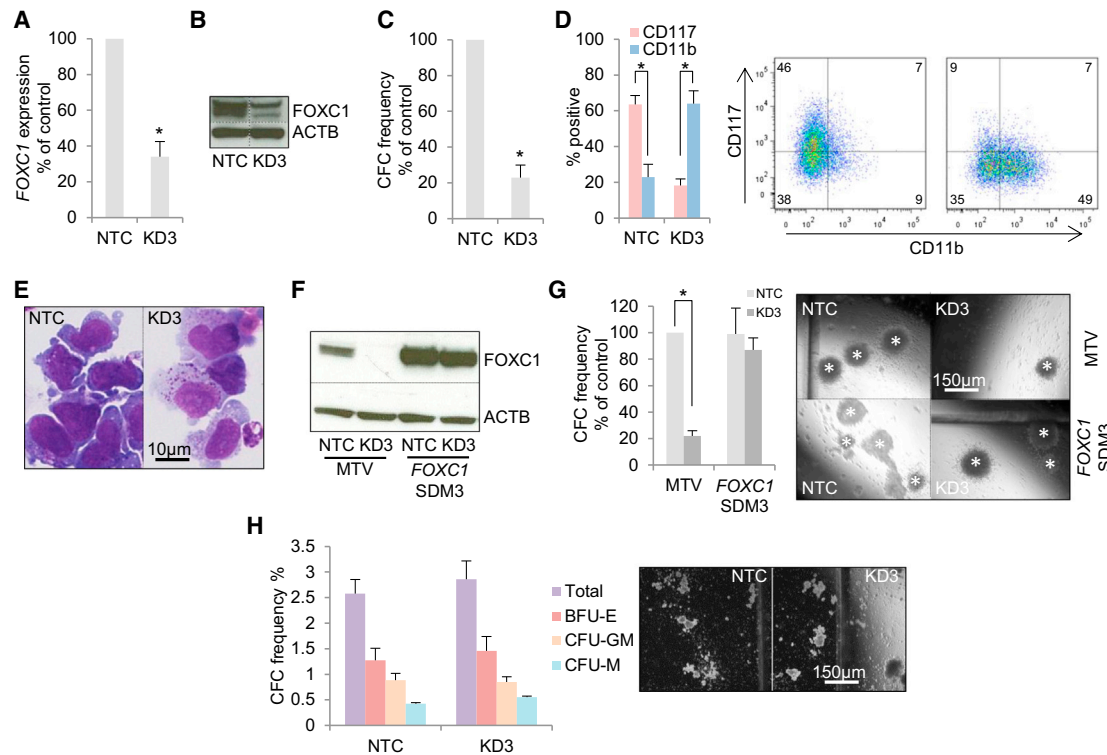


**Figure 2. FOXC1 Sustains the Differentiation Block and Clonogenic Potential of Human AML Cells**

(A–G) Human THP1 AML cells were infected with a lentivirus targeting *FOXC1* for KD (KD3) or a non-targeting control vector (NTC). (A) Bar chart shows mean + SEM relative transcript expression in KD versus control cells ( $n = 3$ ). (B) Western blot shows expression of the indicated proteins in the indicated conditions. (C) Bar chart shows the mean + SEM colony-forming cell (CFC) frequencies of KD cells relative to control cells enumerated after 10 days in semi-solid culture ( $n = 4$ ). (D) Bar chart (left) shows mean + SEM percentage of cells positive for the indicated cell surface markers, as determined by flow cytometry analysis 6 days following the initiation of KD ( $n = 4$ ). Representative flow cytometry plots (right) are also shown. (E) Representative images of cytopins of cells from (D). (F) Western blot shows expression of the indicated proteins in the indicated conditions. (G) Bar chart (left) shows mean + SEM CFC frequencies of THP1 AML cells expressing either *FOXC1* SDM3 (for site-directed mutagenesis #3) or a control retroviral vector (MTV) in *FOXC1* KD cells relative to control cells. Colonies were enumerated after 10 days in semi-solid culture ( $n = 3$ ). Image (right) shows representative colonies, each of which is marked by a white asterisk. (H) Normal human  $CD34^+$  HSPC were infected with the *FOXC1* KD3 vector or a non-targeting control. Bar chart (left) shows mean + SEM total and types of CFCs ( $n = 3$  separate individuals). Colonies were enumerated after 14 days. Image (right) shows representative colonies. BFU-E, burst-forming unit erythroid; CFU-GM, colony forming unit granulocyte/macrophage; CFU-M, colony forming unit macrophage. For (A), (C), (D), and (G),  $*p < 0.05$  by unpaired t test. See also Figure S2.

(Tables S2 and S3). There was no association of high *FOXC1* expression with other recurring mutations in AML (Table S3).

### FOXC1 Sustains Clonogenic Potential and Differentiation Block in AML Cells

To investigate whether *FOXC1* expression in AML contributes functionally to transformation, we performed knockdown (KD) experiments in human THP1 AML cells, which exhibit both a  $t(9;11)$  translocation, the cytogenetic hallmark of *MLL-AF9*, and high *FOXC1* expression. *FOXC1* KD led to loss of clonogenic potential due to induction of differentiation and G1 arrest (Figures 2A–2E and S2A). Following KD, there was downregulation of the stem cell marker CD117, upregulation of the myeloid marker CD11b (Figure 2D), morphological differentiation (Figure 2E), G1 arrest (Figure S2A), and apoptosis (Figure S2B). To confirm that the observed phenotype was an on-target consequence of *FOXC1* KD, similar experiments were performed in a line constitutively expressing a *FOXC1* cDNA engineered by site-directed mutagenesis to generate KD-resistant transcripts. *FOXC1*

forced expression and resistance to KD was confirmed by western blotting (Figure 2F). Expression of KD-resistant *FOXC1* in *FOXC1* KD cells completely prevented loss of clonogenic potential (Figure 2G). KD of *FOXC1* in other *FOXC1* expressing AML cell lines representative of a variety of molecular subtypes gave similar results (Figures S2C and S2D). In contrast, there was no reduction in the clonogenic and multilineage differentiation potential of normal human  $CD34^+$  cells (which do not express *FOXC1*) infected with the same *FOXC1* KD construct (Figure 2H). These data demonstrate that *FOXC1* expression in AML contributes to oncogenic potential by maintaining differentiation block and clonogenic activity.

### Expression of FOXC1 Transiently Impairs Myeloid Differentiation in Normal HSPCs

To investigate the consequences of forced *FOXC1* expression in normal HSPCs, murine  $CD117^+$  BM cells were infected with retroviral vectors (Figure 3A). In serial replating experiments, we observed a significant but transient myeloid differentiation

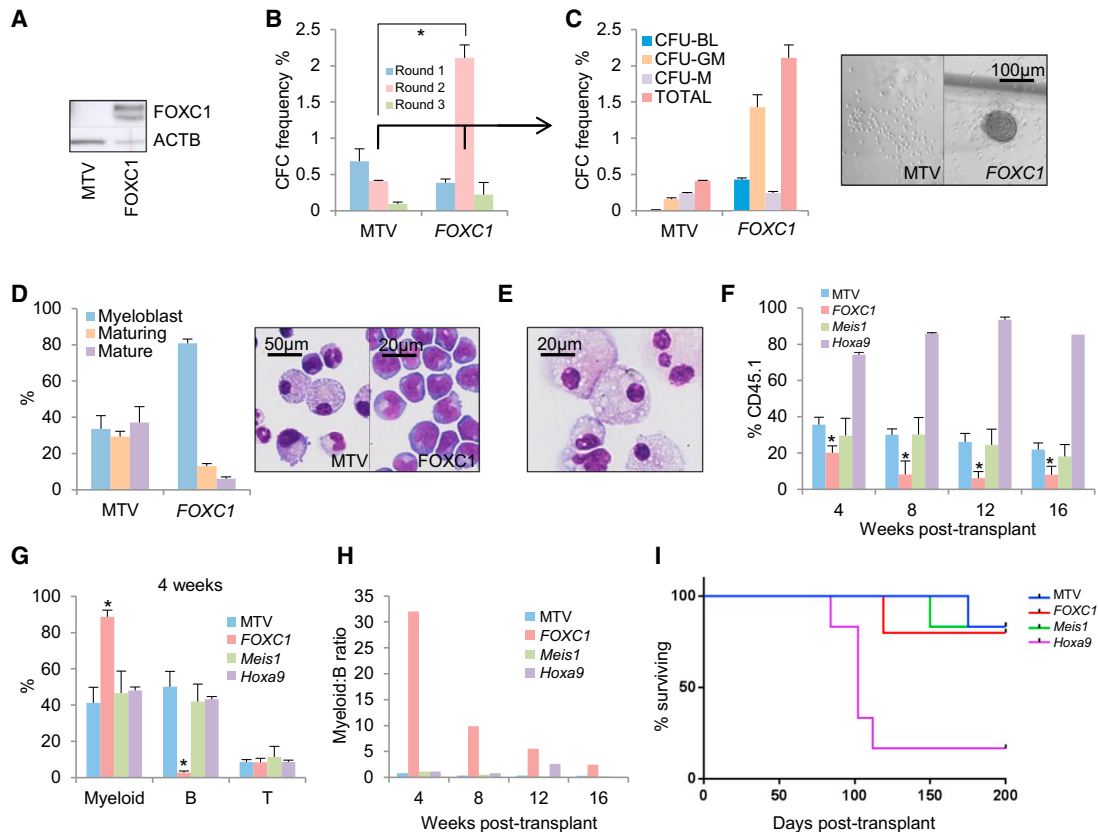


**Figure 3. FOXC1 Transiently Impairs Myeloid Differentiation of Normal HSPCs**

(A–E) Murine CD117<sup>+</sup> BM cells were infected with *FOXC1*-expressing or control retroviral vectors and serially replated in vitro. (A) Western blot shows *FOXC1* expression in CD117<sup>+</sup> BM cells 48 hr following drug selection and 72 hr post-spinoculation. (B) Bar chart shows mean + SEM CFC frequencies at the end of each round of serial replating ( $n = 3$ ). \* $p < 0.001$  by unpaired  $t$  test. (C) Bar chart (left) shows mean + SEM types of colonies formed in the second round of culture ( $n = 3$ ). Image (right) shows representative colonies. (D) Bar chart (left) shows mean + SEM percentage of the indicated cell types in cytopsin preparations from the end of round 1 ( $n = 3$ ). Representative images (right) are shown. (E) Representative cytopsin image of *FOXC1*<sup>+</sup> cells at the end of round 3. (F–I) Murine CD45.1<sup>+</sup> CD117<sup>+</sup> BM cells were infected with the indicated retroviral vectors;  $10^6$  drug-resistant cells were transplanted into CD45.2<sup>+</sup> irradiated congenic recipients 96 hr following spinoculation. (F) Bar chart shows mean + SEM percentage donor-derived CD45.1<sup>+</sup> cells in blood at the indicated times post-transplantation. \* $p < 0.05$  for comparison of *FOXC1*<sup>+</sup> recipients versus all others, and at each time point, by one-way ANOVA with Fisher's least significant difference post hoc test. (G) Bar chart shows mean + SEM percentage contribution of donor-derived cells to the indicated lineages (myeloid-lineage, Gr-1<sup>+</sup> and/or Mac-1<sup>+</sup>; B-lineage, CD19<sup>+</sup>B220<sup>+</sup>; T-lineage, T cell receptor  $\beta$ <sup>+</sup>) 4 weeks post-transplantation. \* $p < 0.001$  for comparison of *FOXC1*<sup>+</sup> recipients versus all others by one-way ANOVA with Fisher's least significant difference post hoc test. (H) Bar chart shows the mean myeloid/B-lineage ratio of donor-derived CD45.1<sup>+</sup> cells in blood at the indicated times post-transplantation. (I) Survival curve of mice transplanted with cells infected with the indicated vectors ( $n = 6$  or 7 mice per cohort). See also Figure S3.

block and enhanced proliferation in *FOXC1*-expressing cells (*FOXC1*<sup>+</sup> cells). In the second round, *FOXC1*<sup>+</sup> cells generated approximately five times as many colonies as did control cells (Figure 3B), with a substantially larger number of tightly packed blast-like colonies and a lower proportion of fully mature macrophage colonies (Figure 3C). In keeping with these observations, *FOXC1*<sup>+</sup> cell populations at the end of the first round contained a higher proportion of myeloblasts versus mature cells (Figure 3D) and a higher proportion of cells in the SG<sub>2</sub>M phase of the cell cycle (Figure S3A). Immunophenotypic analysis demonstrated lower expression of the myeloid differentiation marker Gr1 and the monocyte/macrophage marker F4/80 in *FOXC1*<sup>+</sup> cells by comparison with control cells (Figure S3B). Despite the significant second-round differences, the consequences of *FOXC1* overexpression were only transient because there was no signif-

icant difference in the clonogenic potential of third-round cells, with *FOXC1*<sup>+</sup> cells at the end of that round displaying features of terminal differentiation (Figure 3E).

To investigate the in vivo consequences of *FOXC1* expression in HSPCs, we performed transplantation experiments. Murine CD117<sup>+</sup> HSPCs were infected with retroviral vectors expressing *FOXC1*, *Meis1*, *Hoxa9*, or an empty vector (hereafter referred to as *FOXC1*<sup>+</sup>, *MEIS1*<sup>+</sup>, *HOXA9*<sup>+</sup>, and MTV cells, respectively) and transplanted into irradiated congenic recipients. *Meis1* and *Hoxa9* were chosen as comparators because forced expression of *Meis1* has no effect on BM chimerism, whereas forced expression of *Hoxa9* is sufficient to cause HSC expansion followed by long latency AML (Thorsteinsdottir et al., 2002). Assessment of donor:recipient chimerism in the blood of transplanted mice over 16 weeks demonstrated, as expected, no significant

difference between those receiving MEIS1<sup>+</sup> cells versus MTV cells (Figure 3F). Also as expected, mice receiving HOXA9<sup>+</sup> cells exhibited significantly higher levels of donor:recipient chimerism (Figure 3F). By contrast, at all time points, recipients of FOXC1<sup>+</sup> cells exhibited significantly lower donor:recipient chimerism in blood (the BM was not sampled) (Figure 3F). Four weeks following transplantation, there was donor-derived multilineage engraftment in all cohorts, with proportionately similar levels of myeloid, B, and T lineage engraftment in MEIS1<sup>+</sup>, HOXA9<sup>+</sup>, and MTV recipients. In contrast, in FOXC1<sup>+</sup> recipients, there were significantly higher levels proportionately of myeloid engraftment and lower levels of B lineage engraftment (Figures 3G and S3C). At the later time points (8, 12, and 16 weeks), HOXA9<sup>+</sup> recipients showed progressive expansion of the myeloid compartment and a proportionate reduction in T-lineage engraftment compared with MEIS1<sup>+</sup> and MTV recipients (Figure S3D). FOXC1<sup>+</sup> recipients maintained myeloid skewing of donor-derived cells. Thus, by comparison with MEIS1<sup>+</sup> and MTV control cells, expression of *FOXC1* in HSPCs reduces donor:recipient chimerism in blood and skews differentiation toward the myeloid lineage and away from the B cell lineage (Figure 3H).

In keeping with progressive expansion of the myeloid compartment, and previous reports (Thorsteinsdottir et al., 2002), mice transplanted with HOXA9<sup>+</sup> cells succumbed to AML with a median latency of 103 days (Figure 3I), whereas at the termination of the experiment 200 days post-transplantation, none of the mice from any other cohort had died of a donor-derived hematological neoplasm or exhibited any features thereof in BM analyses (data not shown). The three mice that did die succumbed to recipient origin T cell leukemia (MTV recipient) or recipient origin T cell lymphoma (MEIS1<sup>+</sup> and FOXC1<sup>+</sup> recipients). Taken together, these data indicate that expression of *FOXC1* in HSPCs, although not overtly leukemogenic, is sufficient to induce a transient myeloid differentiation block in vitro and to skew differentiation toward the myeloid lineage in vivo.

### **FOXC1 Expression in Human AML Is Associated with High HOX Gene Expression**

Given that expression of *FOXC1* alone is insufficient to induce AML, we next investigated whether it might collaborate with other factors to promote leukemogenesis. To identify transcription factor genes whose expression is associated with that of *FOXC1* in human AML, we compared *FOXC1*<sup>high</sup> AMLs with *FOXC1*<sup>low</sup> AMLs (Figure S1A and Table S2) (Wouters et al., 2009) and found *HOXA9*, *HOXA5*, and *HOXB3* to be the most highly upregulated genes in the *FOXC1*<sup>high</sup> group (Figure S4A). Notably, high expression of HOX genes is a shared feature of NPM1-mutated AML and AML with a t(6;9) translocation, potentially explaining the particular association of high *FOXC1* expression with these molecular subtypes. Quantitative PCR (Figure 4A) and analysis of expression data (Figures 4B and 4C) confirmed the strong association. By quantitative PCR, all five samples from our cohort with high *FOXC1* expression exhibited high *HOXA9* expression, and 43% of high-*HOXA9*-expressing AML samples exhibited high *FOXC1* expression (Figure 4A). In the published studies, 95 of 100 (95%) and 34 of 36 (94%), respectively, with high *FOXC1* expression also exhibited high *HOXA9* expression (Figures 4B and 4C), and 95 of 320 (30%) and 34 of

115 (30%), respectively, of high-*HOXA9*-expressing AML samples exhibited high *FOXC1* expression (Figures 4B and 4C). Of the total of seven *FOXC1*<sup>high</sup>, *HOXA9*<sup>low</sup> cases from both expression studies, three exhibited high *HOXB2*, *HOXB3*, or *HOXB4* expression, leaving just 4 of 129 (3%) of *FOXC1*<sup>high</sup> cases across both studies lacking HOX gene expression.

To examine this association in more detail, 461 AML cases (Wouters et al., 2009) were grouped into five categories according to their pattern of HOX gene expression (Figure S4B). Twelve HOX genes were expressed at very high level in AML (where at least 1% of 461 samples exhibited probeset values in the top 10% of protein-coding genes, i.e., >log<sub>2</sub> 8.3) and unsupervised analysis of their expression patterns demonstrated three major clusters: *HOXA*, *HOXB2–6*, and *HOXB8/9* (Figure S4C). The karyotypes and mutation spectra of the five groups were as expected (Figures S4D and S4E) (Wouters et al., 2009). The *FOXC1*<sup>high</sup> cases were most strongly associated with HOX group 1 (pan-HOX<sup>high</sup>) and to a lesser extent with HOX groups 2 (*HOXA*<sup>high</sup>/*HOXB2–6*<sup>high</sup>/*HOXB8–9*<sup>low</sup>) and 3 (*HOXA*<sup>high</sup>/*HOXB*<sup>low</sup>) (Figure S4F). This indicates that *FOXC1* expression in AML is strongly associated with high-level expression across the *HOXA* and *HOXB* locus, not just *HOXA9*. The observation that approximately 30% of *HOXA9*-expressing human AML samples express *FOXC1* in a tissue-inappropriate manner suggested that *FOXC1* collaborates with HOX family transcription factors to enhance leukemogenesis.

### **FOXC1 Expression Collaborates with Hoxa9 Expression to Enhance Clonogenic Potential and Differentiation Block and Accelerate the Onset of Symptomatic Leukemia**

To investigate this question further, murine CD117<sup>+</sup> HSPCs were infected in pairwise combinations with retroviral vectors expressing *Hoxa9*, *FOXC1*, *Meis1*, or a control vector (to generate *Hoxa9*/MTV, *Hoxa9*/*FOXC1*, and *Hoxa9*/*Meis1* cells, respectively), and their clonogenic potential was assessed in serial replating assays. MEIS1 is an established *HOXA9* cofactor (Kroon et al., 1998). As expected, *Hoxa9* expression induced sustained clonogenic activity of BM HSPCs in serial replating assays, an effect enhanced by *Meis1* (Figure 4D). Interestingly, co-expression of *FOXC1* with *Hoxa9* significantly enhanced the clonogenic activity of BM HSPCs versus cells expressing *Hoxa9* alone (Figure 4D). *Hoxa9*/*FOXC1* co-expression also significantly enhanced differentiation block by comparison with cells expressing *Hoxa9* alone: by the fourth round of culture, *Hoxa9*/*FOXC1* cells formed approximately four times more type I colonies (which contain poorly differentiated myeloid cells) (Figures 4D–4F), displayed more blast cells in cytospin preparations (Figure 4G), and expressed significantly lower levels of both the mature myeloid marker Gr1 and the monocyte/macrophage marker F4/80 (Figures 4H and 4I).

To determine whether *HOXA9* and *FOXC1* collaborate in leukemogenesis, *Hoxa9*/MTV, *Hoxa9*/*FOXC1*, and *Hoxa9*/*Meis1* double-transduced HSPCs were transplanted into irradiated congenic recipients. Levels of donor:recipient chimerism in blood at 4 and 8 weeks post-transplantation were lower in *Hoxa9*/*FOXC1* recipients than in the other two cohorts (Figure 5A). Donor-derived multilineage engraftment was observed in all three cohorts at both time points (Figures 5B and S5A).

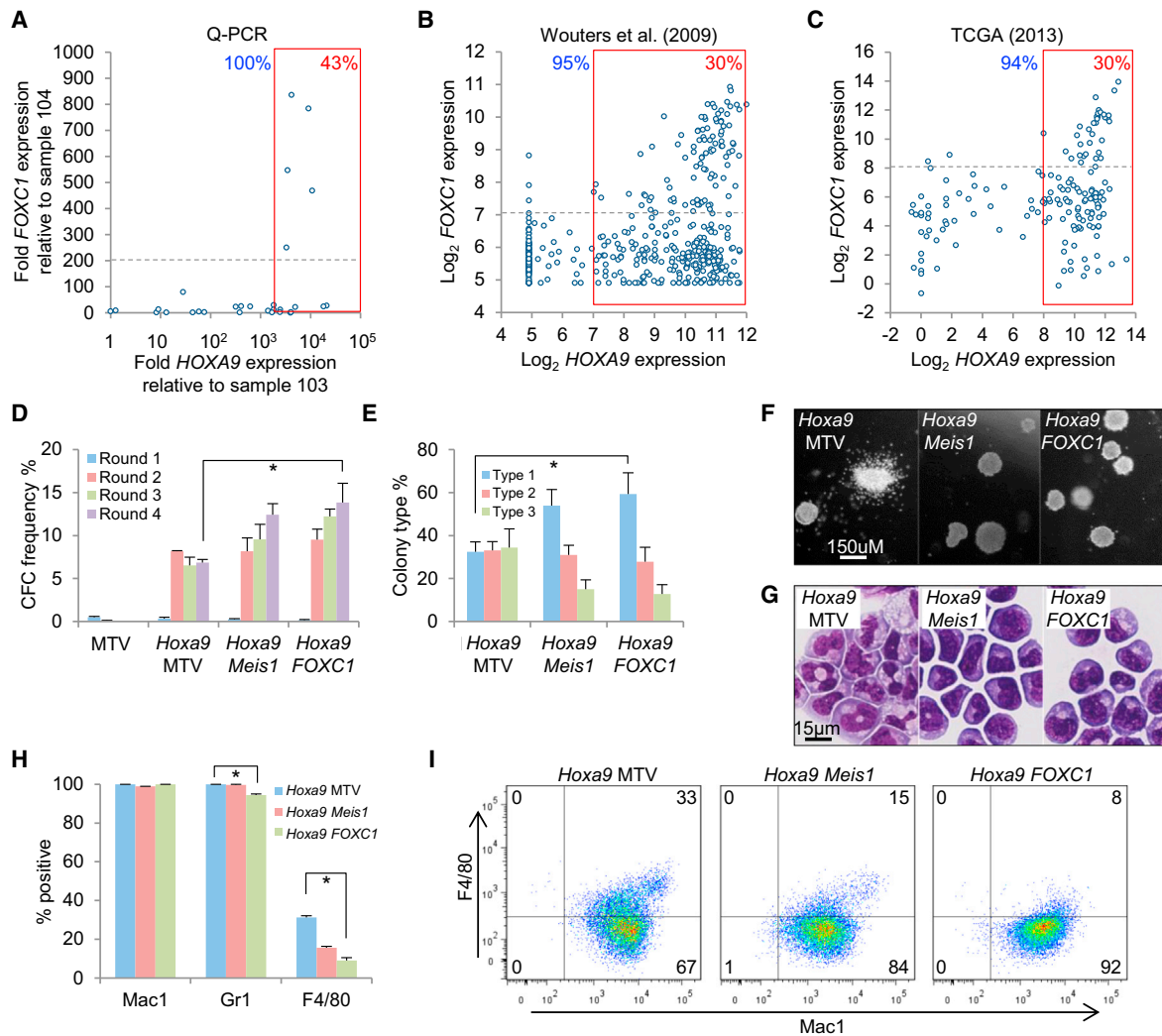


**Figure 4. *FOXC1* Collaborates with *HOXA9* to Enhance Clonogenic Potential and Differentiation Block in BM HSPCs**

(A–C) Scatterplots show the expression of *FOXC1* versus *HOXA9* in primary AML patient samples as determined by (A) quantitative PCR ( $n = 29$ ; see also Table S1) or (B and C) array expression values from the indicated studies. Percentages in blue text indicate proportion of *FOXC1*<sup>high</sup> samples exhibiting high *HOXA9* expression. Percentages in red text indicate the proportion of *HOXA9*<sup>high</sup> samples (in the red box) additionally exhibiting high *FOXC1* expression (above the dotted gray line).

(D) Bar chart shows mean + SEM CFC frequencies after each round of serial replating of murine CD117<sup>+</sup> BM cells co-transduced with the indicated retroviral or control expression vectors ( $n = 3$ ).

(E) Bar chart shows mean + SEM frequencies of colony types after the fourth round of serial replating ( $n = 3$ ). Type I colonies contain poorly differentiate myeloblasts, type II colonies contain a mixed population of blasts and differentiating myeloid cells, and type III colonies contain terminally differentiated myeloid cells. For (D) and (E), \* $p < 0.05$  by one-way ANOVA with Fisher's least significant difference post hoc test.

(F and G) Representative images show (F) colonies and (G) cytopsin preparations from the end the fourth round of replating.

(H) Bar chart shows mean + SEM percentage of cells positive for the indicated cell surface markers (as determined by flow cytometry) following 6 days in liquid culture ( $n = 3$ ). \* $p < 0.001$  by one-way ANOVA with Fisher's least significant difference post hoc test.

(I) Representative flow cytometry plots of cells shown in (H).

See also Figure S4.

However, as with the single transduction transplants (Figures 3G and 3H), there were significantly higher levels proportionately of myeloid engraftment, and lower levels of B-lymphoid engraftment, among recipients of *Hoxa9/FOXC1* cells by comparison with mice receiving either *Hoxa9/MTV* or *Hoxa9/Meis1* cells (Figures 5B, 5C, and S5A).

As expected, recipients of *Hoxa9/Meis1* cells developed AML more rapidly than recipients of *Hoxa9/MTV* cells (median 57

versus 125 days; Figure 5D). Strikingly, despite lower donor:recipient chimerism in the blood in the initial post-transplantation period, recipients of *Hoxa9/FOXC1* cells also succumbed to AML substantially earlier than mice receiving *Hoxa9/MTV* cells (83 versus 125 days; Figure 5D). By comparison with *Hoxa9/MTV* or *Hoxa9/Meis1* recipients, at the point of death, *Hoxa9/FOXC1* recipients exhibited significantly lower total circulating leukocyte counts, although 30%–40% of these were blasts

(Figures 5E, 5F, and S5B). However, *Hoxa9/FOXC1* recipients exhibited much more extensive tissue infiltration with blasts than mice from other cohorts, with high-level donor:recipient chimerism in BM and spleen (Figures S5C and S5D). Thus, a key feature of the *Hoxa9/FOXC1* murine AMLs was failure of AML blasts to mobilize substantially to the blood despite high-level involvement of BM, liver, and spleen. In the BM, *Hoxa9/FOXC1* recipients exhibited significantly higher blast percentages, significantly higher CD117 expression, and significantly lower F4/80 expression (Figures 5G–5J). In each cohort and in each case, autopsy demonstrated splenomegaly and hepatomegaly, with spleen weights being significantly higher in *Hoxa9/FOXC1* recipients than both other cohorts and liver weights being significantly higher in *Hoxa9/FOXC1* recipients versus *Hoxa9/Meis1* recipients (Figure S5D). Histological analysis of spleen demonstrated that in *Hoxa9/MTV* and *Hoxa9/Meis1* recipients, the splenic architecture was maintained with preservation of the white pulp. The red pulp, however, was expanded by sheets of blast cells, with scattered normal megakaryocytes and erythroid precursors indicating residual but extramedullary hematopoiesis. By comparison, in *Hoxa9/FOXC1* recipients, the splenic architecture was completely effaced by blasts (Figure S5E). In the livers of *Hoxa9/MTV* and *Hoxa9/Meis1* recipients, there was periportal and perivenular accumulation of blasts, more extensive in the former than the latter, with relative sparing of the intervening parenchyma, where only single and small groups of blasts were seen within sinusoids. By contrast, in *Hoxa9/FOXC1* recipients, there was a diffuse infiltrate of blasts, forming small clusters that expanded the sinusoids. Periportal and perivenular blasts, although present, were less conspicuous than those seen in mice from the other cohorts (Figures S5F and S5G). Cell-cycle analysis of AML cells from both BM and spleen demonstrated a significantly higher fraction of cycling cells in *Hoxa9/FOXC1* recipients by comparison with the other cohorts, consistent with a differentiation block at a proliferative progenitor stage (Figures 5K, 5L, and S5H). FOXC1 protein was expressed in the *Hoxa9/FOXC1* AML cells (Figure S5I), which were also able to initiate leukemia in secondarily transplanted recipients with shortened latency (Figure 5M).

Together, these *in vitro* and *in vivo* data demonstrate that FOXC1 collaborates with HOXA9 to increase clonogenic potential and cell-cycle progression, enhance a monocyte/macrophage and B-lineage lineage differentiation block and accelerate the onset of symptomatic leukemia in mice.

### FOXC1 Represses a Monocytic Lineage Differentiation Program in Leukemic Hematopoiesis

To investigate the consequences of FOXC1 expression on the transcriptome in murine AML, we next performed exon array analysis using flow-sorted CD117<sup>+</sup>Gr1<sup>+</sup> leukemia cells recovered from sick mice. Populations with this immunophenotype are enriched for leukemia-initiating cell activity in *Hoxa9/Meis1* murine leukemias (Gibbs et al., 2012). In keeping with the observed immunophenotypes of the respective leukemias (Figures 5I and 5J), analysis of protein-coding genes that passed threshold criteria demonstrated that *Hoxa9/FOXC1* AMLs clustered separately from *Hoxa9/Meis1* and *Hoxa9/MTV* AMLs (which clustered much more closely with one another) (Figure S6A). Genes with the highest mean differential expression

(at least 2-fold) in *Hoxa9/FOXC1* AMLs versus the others formed two groups: group A genes, which were more highly expressed in the *Hoxa9/FOXC1* AMLs versus the others, and group B genes (the larger set), which were repressed (Figure 6A and Table S4). Gene ontology analysis demonstrated significant enrichment within the group B gene set of biological process terms such as “immune response,” “defense response,” and “inflammatory response” (Table S4), indicating a gene set associated with myeloid cells involved in inflammation and immunity. At a similar level of statistical significance, there were no enriched terms among the group A gene set.

To determine whether FOXC1-regulated gene sets in murine AML cells were more highly expressed in monocytes or neutrophils, we evaluated the relative expression of human homologs of group A and B genes in exon array data sets from primary human cells using gene set enrichment analysis (GSEA) (Table S5). In keeping with reduced expression of the monocyte/macrophage marker F4/80 in murine *Hoxa9/FOXC1* AML cells (Figures 5I and 5J), this cross-species analysis demonstrated that FOXC1 repressed a monocyte-expressed gene set and promoted expression of a neutrophil-expressed gene set (Figure 6B). Also in keeping with the unexpected ability of the mesenchyme-expressed transcription factor FOXC1 to repress monocyte differentiation, we observed that phorbol ester treatment of HL60 AML cells (which express FOXC1) led to substantial downregulation of the protein as cells underwent monocytic differentiation, whereas the reverse was the case as cells underwent granulocytic differentiation following all-trans retinoic acid treatment (Figure S6B).

Next, to determine whether a signature of FOXC1 transcriptional activity could be identified in human AML, and to confirm the functional relevance of its derepression in human disease, we evaluated the expression of human homologs of FOXC1-repressed group B genes in AML using GSEA (Figure 6A and Table S4). Protein-coding genes in FOXC1<sup>high</sup> AMLs versus FOXC1<sup>low</sup> AMLs (Wouters et al., 2009) were ranked using a signal-to-noise ranking metric (Table S5). GSEA demonstrated highly significant negative enrichment of FOXC1-repressed group B genes among FOXC1<sup>high</sup> AMLs versus FOXC1<sup>low</sup> AMLs, and this was observed whether all AMLs were considered (Figure 6C; n = 461) or just those expressing HOXA9 (Figure 6D; n = 320). In fact, in leading edge analyses (Table S4), there was a highly significant association of higher FOXC1 expression with greater repression of group B genes (Figure 6E). Remarkably, when the morphological classification of HOXA9<sup>+</sup> AMLs was considered, among cases with high FOXC1 expression, there were significantly fewer AMLs of French-American-British (FAB) M4 and M5 subtypes, which exhibit monocytic differentiation, and significantly more of the FAB M2 subtype, which lack it (Figure 6F). Furthermore, in this cohort of younger adult AML patients (aged < 60 years) treated intensively on the Dutch HOVON protocols, those with FOXC1<sup>high</sup> AML exhibited significantly inferior survival in comparison with FOXC1<sup>low</sup> cases, whether all other AMLs were considered (median 12 versus 32 months) or only those expressing HOXA9 (median 12 versus 20 months) (Figure 6G). Indeed, in multivariate analysis (Table S6), high FOXC1 expression was an independent predictor of inferior survival in addition to age, cytogenetic risk score, and NPM1/FLT3 mutation status, whether analyzed as a categorical variable

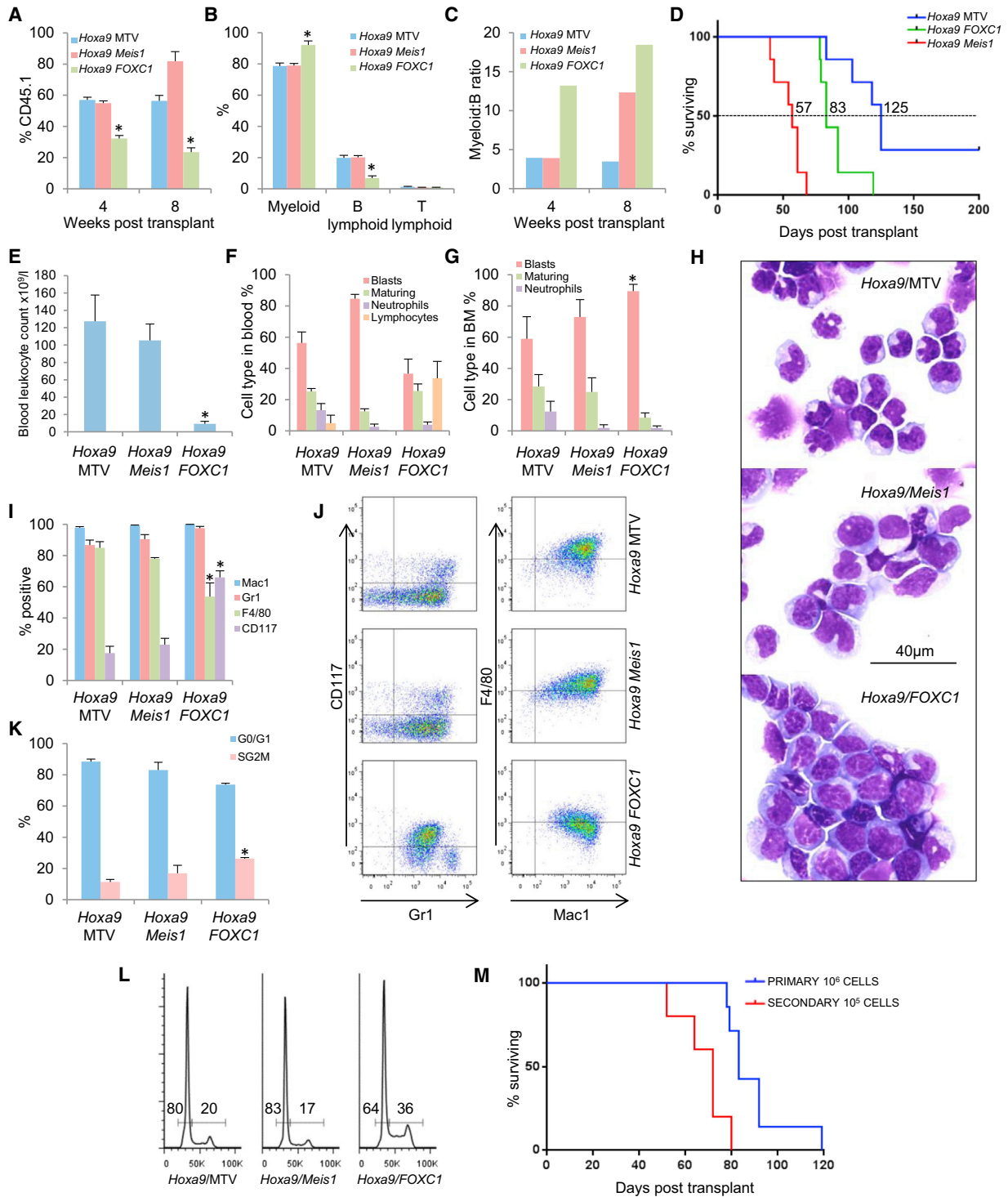


**Figure 5. FOXC1 Collaborates with HOXA9 to Accelerate Leukemogenesis**

Murine CD45.1<sup>+</sup> CD117<sup>+</sup> BM cells were co-transduced with retroviral vectors. Ninety-six hours later, 10<sup>6</sup> drug-resistant cells were transplanted into CD45.2<sup>+</sup> irradiated congenic recipients.

(A) Bar chart shows mean + SEM percentage of donor-derived CD45.1<sup>+</sup> cells in blood at the indicated times post-transplantation.

(B) Bar chart shows mean + SEM percentage contribution of donor-derived cells to each lineage in blood 4 weeks post-transplantation.

(C) Bar chart shows the mean myeloid/B-lineage ratio of donor-derived cells in blood at the indicated times post-transplantation.

(D) Survival curves of transplanted mice (n = 7 per cohort). Median survivals are shown.

(legend continued on next page)

(Table S6) or a continuous variable (hazard ratio 1.136, 95% confidence interval 1.04–1.24;  $p = 0.004$ ; rest of model not shown). These data indicate that in human leukemic hematopoiesis, as in murine leukemic hematopoiesis, expression of *FOXC1* enhances a block to monocyte/macrophage differentiation and leads to inferior survival.

#### FOXC1 Regulates Expression of *KLF4*

The transcription factor *KLF4* positively regulates monocyte differentiation (Feinberg et al., 2007) and exhibits anti-proliferative and tumor suppressor activity in B cell malignancies (Kharas et al., 2007). Consistent with our observation that *FOXC1* expression is inversely associated with monocytic morphologic classification of human AML (Figure 6F) (Wouters et al., 2009), *KLF4* expression was significantly lower in *FOXC1*<sup>high</sup> human AML versus *FOXC1*<sup>low</sup> AML (Figure 7A). *Klf4* expression was also significantly lower in murine *Hoxa9/FOXC1* AMLs in comparison with *Hoxa9/MTV* and *Hoxa9/Meis1* AMLs (Figure 7B). Functionally, in human THP1 AML cells, *FOXC1* KD led to *KLF4* upregulation (Figure 7C), and in murine CD117<sup>+</sup> HSPCs, forced expression of *FOXC1* reduced *Klf4* expression, had no effect on expression of *Hoxa9*, and modestly increased *Meis1* expression (Figure 7D). Forced expression of *KLF4* in murine *Hoxa9/FOXC1* AML cells significantly reduced both clonogenic cell frequencies and colony size (Figures 7E–7G) through reduction of the proportion of cells in the SG<sub>2</sub>M phase of the cell cycle. These data suggest that direct or indirect repression of *KLF4* by *FOXC1* is one significant contributing factor to the phenotypic appearances of murine and human *FOXC1*<sup>+</sup> AMLs.

#### Loss of Polycomb-Mediated Repression Promotes *FOXC1* Derepression

In normal human CD34<sup>+</sup> HSPC, the *FOXC1* gene occupies a DNA-hypomethylated and histone H3K27-trimethylated region of the genome (Figures 8A and S7A) (Zhou et al., 2011). Interestingly, despite absent or very low level expression, the locus exhibits hypersensitivity to DNase treatment, as well as the presence of histone H3K4 methylation marks and acetylation of H2A, H2B, H3, and H4 histones, suggesting a lack of chromatin compaction (Figures 8A and S7A). In K562 leukemia cells, *FOXC1* is also not expressed and sits in chromatin with similar features to that seen in CD34<sup>+</sup> cells. Importantly, there is significant binding of Polycomb repressive complex (PRC) 2 components EZH2 and SUZ12 across the locus correlating with the presence of H3K27 trimethyl marks. In addition, there are also co-localized binding peaks of PRC1 components RNF2, CBX2,

and CBX8 (Figure S7B). In HeLa cells in which *FOXC1* is expressed, EZH2 binding to the locus is absent (Figure S7C). These data raise the possibility that in normal hematopoietic cells, transcriptional silence of *FOXC1* is maintained by PRC.

To address this, we treated normal human CD34<sup>+</sup> cells from multiple donors with PRC inhibitors. Cells treated with the EZH2 inhibitor GSK343 (Verma et al., 2012) exhibited a significant increase in expression of *FOXC1* but not *HOXA9*, which lacks significant H3K27 trimethylation in CD34<sup>+</sup> cells (Figures 8A and 8B). In separate experiments, cells treated with UNC1999, a dual EZH1 and EZH2 inhibitor (Konze et al., 2013), exhibited a more extensive fold increase in *FOXC1* expression, but again, expression of *HOXA9* was unaffected. PRT4165, a PRC1 E3 ubiquitin ligase inhibitor (Ismail et al., 2013), modestly enhanced *FOXC1* but not *HOXA9* expression (Figure 8C). These data indicate that continued repression of *FOXC1* in the hematopoietic system is mediated by PRC2 and imply that loss of its activity at this genomic locus contributes to its derepression in AML.

To ascertain whether derepression of silenced, Polycomb-marked transcription factor genes is widespread in AML or a locus-specific phenomenon, we identified the set of transcription factor genes exhibiting a similar epigenetic and transcriptional pattern to *FOXC1* in normal CD34<sup>+</sup> cells (i.e., minimally or not expressed and with high H3K27 trimethylation) using ENCODE data ( $n = 253$  genes; Table S7) (Zhou et al., 2011). Of the 230 genes represented by probesets on the U133 Plus 2.0 array, only three (*IRX3*, *IRX5*, and *HOXB8*) were both expressed significantly in AML (i.e., in the top 20% of probesets in at least 5% of 461 cases) and unexpressed in mature blood cell lineages (as determined by RNA sequencing of peripheral blood mononuclear cells; Zhou et al., 2011). The Iroquois homeobox factors *IRX3* and *IRX5* have roles in skeletal, cardiac and neural development. Although there was a strong positive association of increased expression of each of these factors with high *FOXC1* expression (Figures 8D, S7D, and S7E), and in particular *IRX3* (Figure 8E), the correlation was not absolute. Thus, tissue-inappropriate expression of *FOXC1* in human AML is a locus-specific phenomenon rather than part of a generalized failure of Polycomb-mediated silencing of repressed genes.

Finally, we considered the possibility that *FOXC1* derepression might be associated with mutations in Polycomb complex components, or intergenic mutations close to *FOXC1* that introduce an enhancer element, as has recently been reported for *TAL1* in T-acute lymphoblastic leukemia (Mansour et al., 2014). There was no association of *FOXC1* expression in AML with

(E and F) Bar charts show mean + SEM (E) total blood leukocyte count and (F) percentage leukocyte type in blood at death in the indicated cohorts, as determined by hemocytometer counting and morphologic analysis of blood smears respectively ( $n = 3-5$  per cohort).

(G) Bar chart shows mean + SEM percentage cell type in BM at death ( $n = 3-5$  per cohort).

(H) Representative images from (G).

(I) Bar chart shows the mean + SEM percentage of donor-derived cells positive for the indicated cell surface markers in BM of leukemic mice, as determined by flow cytometry.

(J) Representative flow cytometry plots from (I).

(K) Mean + SEM percentage of BM cells in the indicated phase of the cell cycle at death.

(L) Representative profiles from (K).

(M) Survival curves of sub-lethally (4.5 Gy) irradiated mice secondarily transplanted with  $10^5$  *Hoxa9/FOXC1* AML cells. Results of primary transplantations of  $10^6$  cells are shown for comparison.

For (A), (B), (E), (G), (I), and (K),  $*p < 0.01$  by one-way ANOVA with Fisher's least significant difference post hoc test for comparison of *FOXC1*<sup>+</sup> samples versus each of the others. See also Figure S5.

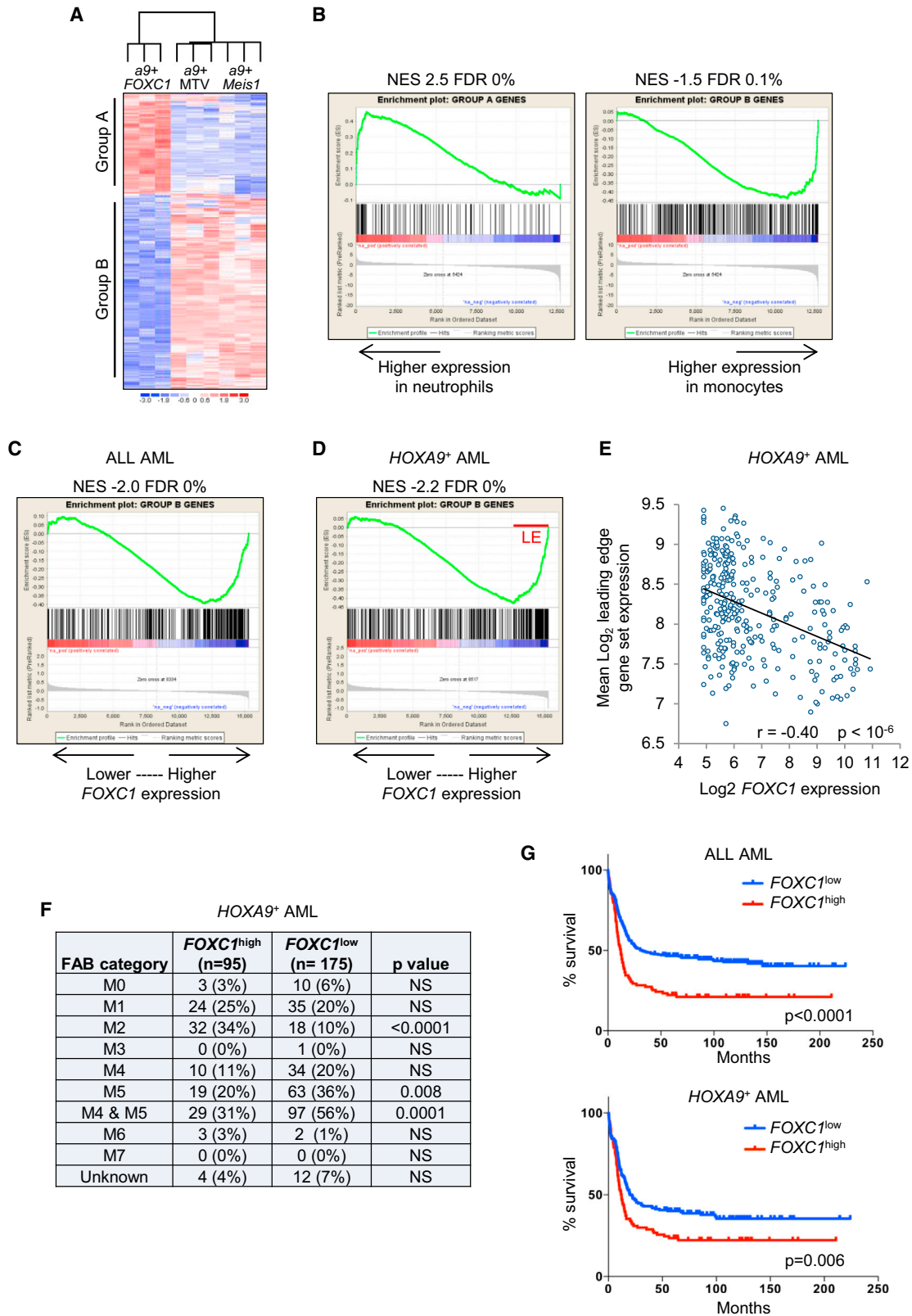


**Figure 6. FOXC1 Represses a Monocyte/Macrophage Differentiation Program in Murine and Human AML**

(A) Cluster analysis of 567 protein-coding genes that passed threshold criteria (expressed [ $\log_2$  expression value > 4.1] and with significantly different expression levels [ $p < 0.05$ , unpaired t test and >2-fold difference] in at least one of the two pairwise comparisons between *Hoxa9*/*FOXC1* AMLs versus the others.

(legend continued on next page)

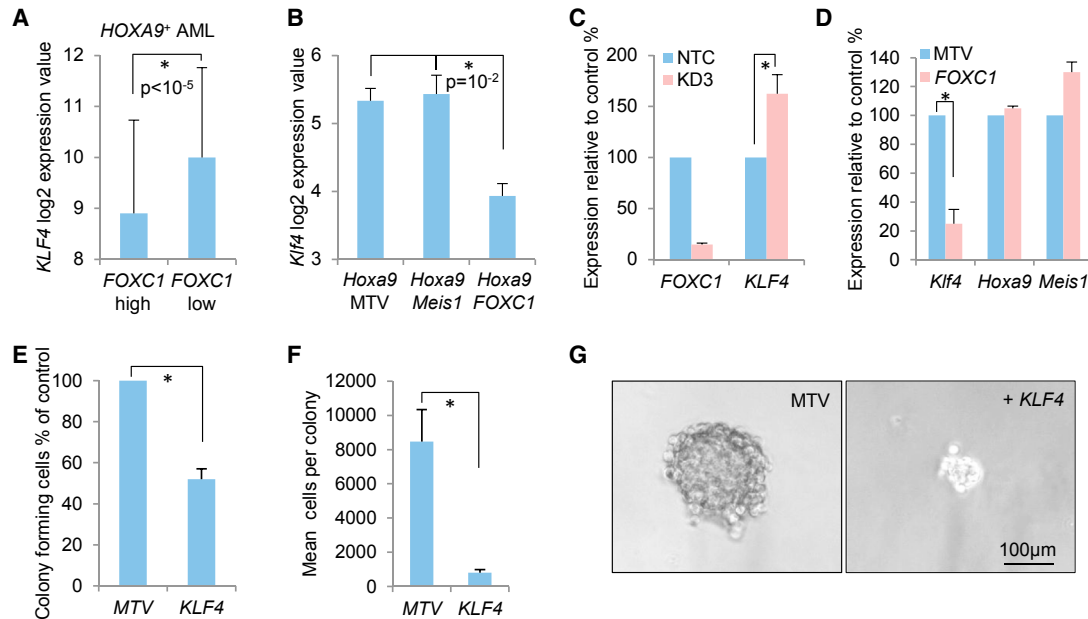


### Figure 7. FOXC1 Regulates KLF4

(A and B) Bar charts show (A) mean + SD log<sub>2</sub> array expression value for *KLF4* in HOXA9-expressing *FOXC1*<sup>high</sup> (n = 95) and *FOXC1*<sup>low</sup> (n = 175) human AML cases from Wouters et al. (2009) and (B) mean + SEM log<sub>2</sub> array expression values for *Klf4* in the indicated murine leukemias (n = 3 per cohort). Statistical significance was assessed using respectively an unpaired t test or one-way ANOVA with Fisher's least significant difference post hoc test.

(C) Bar chart shows mean + SEM relative expression of the indicated genes 72 hr after initiation of *FOXC1* KD using construct KD3 or an NTC (n = 3) (see also Figure 2).

(D) Bar chart shows mean + SEM relative expression of the indicated genes 72 hr after retroviral infection of CD117<sup>+</sup> HSPCs with *FOXC1*-expressing or control retroviral vectors and 48 hr following drug selection (n = 3) (see also Figure 3).

(E–G) *Hoxa9*/*FOXC1* AML cells were infected with *KLF4*-expressing or control retroviral vectors and cultured in semi-solid medium. Bar charts show (E) mean + SEM relative CFC frequencies and (F) mean + SEM cells per colony in *KLF4*-expressing cells versus controls (n = 3).

For (C)–(F), \*p < 0.05 with an unpaired t test for the indicated comparisons. (G) Representative image from (E).

mutations in PRC1 or PRC2 components (Table S8), and comparison of whole-genome sequencing data (Cancer Genome Atlas Research Network, 2013) from six patients with high *FOXC1* expression versus six with absent *FOXC1* expression revealed no genomic loci ± 1 MB from the transcription start site of *FOXC1* that were consistently altered either by indels or single-nucleotide variations in either group (Table S9). This indicates that derepression of *FOXC1* in AML is not driven by genetic mutation of Polycomb components or *FOXC1* local regulatory regions.

## DISCUSSION

Derepression of *FOXC1* is a frequent phenomenon in human AML, with approximately 20% of cases exhibiting significant levels of expression (Wouters et al., 2009). Observed frequencies

were higher still in studies focused on the AML stem and progenitor compartment (Saito et al., 2010; Kikushige et al., 2010; Goardon et al., 2011). More specifically, in bulk AML samples, high *FOXC1* expression is seen in ~40% of patients with an *NPM1* mutation and ~50% of those with dual *NPM1* and *FLT3*-ITD mutations (Wouters et al., 2009). The overall frequency of high *FOXC1* expression in human AML exceeds significantly the frequency of mutations in, for example, *IDH1* and *IDH2* and translocations affecting *MLL*.

Differentiation block is a characteristic feature of AML, and the consequence of derepressed *FOXC1* expression is to enhance monocyte/macrophage and B cell lineage blocks, as evidenced by our murine and human functional studies and our bioinformatics analyses. The observation that *FOXC1*<sup>high</sup> human AMLs are less likely to exhibit monocytic lineage morphologic classifications (i.e., FAB-M4 and M5) and more likely to exhibit

(B–D) GSEA plots show analyses of enrichment of human homologs of group A and/or group B genes in protein-coding gene lists ranked using a signal-to-noise metric according to expression in (B) primary human neutrophils versus primary human monocytes, (C) *FOXC1*<sup>high</sup> (n = 100) versus *FOXC1*<sup>low</sup> (n = 290) primary AML samples (Wouters et al., 2009), or (D) HOXA9-expressing *FOXC1*<sup>high</sup> (n = 95) versus *FOXC1*<sup>low</sup> (n = 175) primary AML samples.

(E) Scatterplot shows expression of *FOXC1* versus mean log<sub>2</sub> expression for the leading edge gene set shown in (D) (see also Table S4) in HOXA9-expressing AML (n = 320).

(F) Analysis of morphological classification of HOXA9-expressing *FOXC1*<sup>high</sup> (n = 95) versus *FOXC1*<sup>low</sup> (n = 175) primary AML samples. Statistical significance for the indicated comparisons was assessed using Fisher's exact test.

(G) Survival curves of patients with *FOXC1*<sup>high</sup> versus *FOXC1*<sup>low</sup> AML.

See also Figure S6 and Tables S4, S5, and S6.

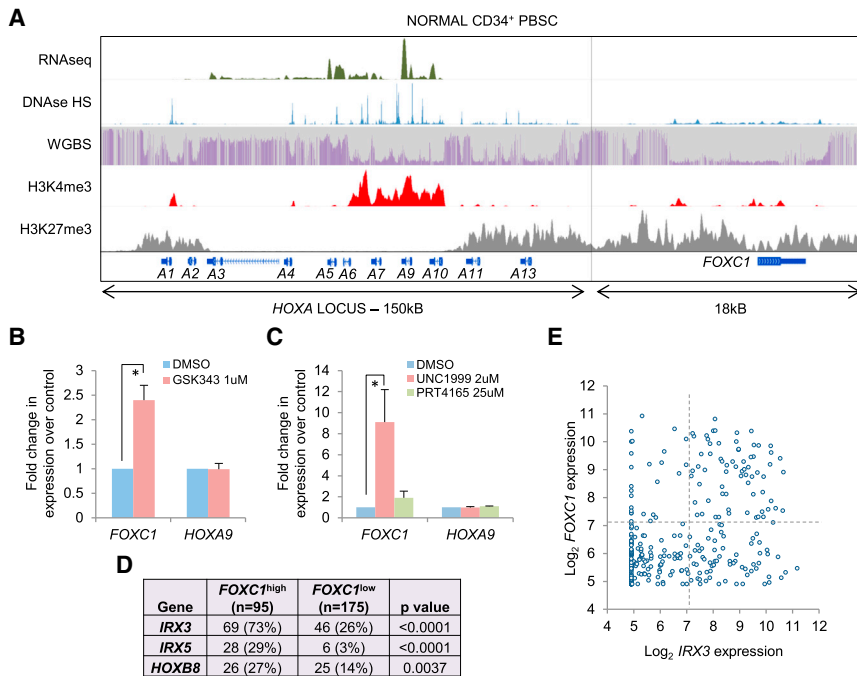


**Figure 8. Derepression of *FOXC1* in Normal *CD34*<sup>+</sup> Cells Is Induced by PRC Inhibition**

(A) Image shows high-throughput sequencing tracks from the ENCODE consortium for the *HOXA* locus and *FOXC1*.

(B and C) *CD34*<sup>+</sup> cells from separate normal donors (n = 3 and 4, respectively) were treated for 4 or 5 days respectively with PRC inhibitors in serum-free liquid culture. Graphs show expression of *FOXC1* and *HOXA9* following treatment with the indicated inhibitors.

(D) Table shows numbers of *HOXA9*-expressing *FOXC1*<sup>high</sup> and *FOXC1*<sup>low</sup> AML cases from Wouters et al. (2009), which also expressed *IRX3*, *IRX5*, or *HOXB8* (at log<sub>2</sub> expression value > 7.1). Statistical significance for the indicated comparisons was assessed using Fisher's exact test.

(E) Scatterplot shows expression of *FOXC1* versus *IRX3* in 320 cases of *HOXA9*-expressing AML. See also Figure S7 and Tables S7, S8, and S9.

morphological classifications associated with granulocyte differentiation (i.e. FAB-M2) is particularly significant and suggests that derepressed *FOXC1* influences morphologic differentiation in human AML.

The near exclusive association of high *FOXC1* expression with high *HOXA/B* locus expression in human AML suggests that *FOXC1* collaborates with *HOX* to enhance leukemogenesis. This suggestion is confirmed by our murine in vitro and in vivo analyses, which show that co-expression of *FOXC1* with *Hoxa9* enhances clonogenic potential and proliferation, significantly shortens leukemic latency, and generates leukemias with pathologic features that are distinct from those seen in *Hoxa9/MTV* and *Hoxa9/Meis1* AMLs. Critically, patients exhibiting high *FOXC1* expression levels also exhibit inferior survival, emphasizing the prognostic significance of derepression at this locus. The association of *FOXC1* expression with *HOX* locus expression implies either that *FOXC1* only exerts its phenotypic effects in the presence of *HOX* or that *HOX* transcription factors are required for expression of *FOXC1*, or both. In favor of the former are our observations that forced expression of *FOXC1* in murine *CD117*<sup>+</sup> HSPC fails to upregulate *Hoxa9* expression and induces only a transient myeloid differentiation block with enhanced clonogenic potential. In this setting, presumably as *HOX* gene expression is downregulated during the course of normal differentiation, *FOXC1* loses its collaborating partner(s) and the phenotype is extinguished. By contrast in AML, where *HOX* gene expression is sustained through multiple mechanisms, *FOXC1* exerts its phenotypic effects continuously. Of note, the cyclin-dependent kinase inhibitor gene *CDKN1A* (coding for p21) is one of the group B genes repressed by *FOXC1* in murine leukemias, suggesting a potential mechanism for the enhanced clonogenic potential of *Hoxa9/FOXC1* double-transduced cells and accelerated onset of AML. It is interesting that *FOXC1* expression in AML collaborates with the consequence of a num-

ber of distinct genetic mutations (i.e., high-level *HOX* gene expression) rather than any specific mutation subset in exclusivity.

Our observations that *FOXC1* blocks monocytic lineage (and in vivo B-lineage) differentiation, and that it collaborates with *HOXA9* to enhance clonogenic potential, emphasize that derepression of this mesenchymal transcription regulator in the hematopoietic system has hematologic rather than mesenchymal consequences. This is despite its lack of expression in normal hematopoiesis. There was, for example, no whole-scale upregulation of a mesenchymal gene program in the *Hoxa9/FOXC1* murine AMLs, although *Vcam1* was one notable exception (Table S4). Expression of this vascular adhesion molecule may explain the relative failure of murine *Hoxa9/FOXC1* AML cells to mobilize to the blood by comparison with *Hoxa9/MTV* and *Hoxa9/Meis1* AML cells. Indeed some genes, such as *FN1* and *VIM*, which are induced by ectopic *FOXC1* expression in breast cancer cells (Bloushtain-Qimron et al., 2008), are repressed by *FOXC1* in murine leukemia cells. Our findings differ significantly from observations in solid tumors such as those of the liver, pancreas, and breast, in which *FOXC1* has been causally implicated in promotion of the epithelial-to-mesenchymal transition characteristic of metastasis (Bloushtain-Qimron et al., 2008; Xia et al., 2013; Yu et al., 2013). In these studies, induced *FOXC1* expression has the expected activity of a mesenchymal regulator: promotion of mesenchymal cellular phenotypes such as enhanced migration, invasion, and metastasis. In AML, by contrast, tissue-inappropriate expression of *FOXC1* interferes with normal tissue activity by blocking differentiation and enhancing proliferation rather than conferring on it a mesenchymal phenotype.

This raises the question as to how *FOXC1* blocks monocytic differentiation in AML. One possibility is that it acts as a dominant-negative inhibitor of one or more forkhead transcription factors whose normal function is to promote monocyte differentiation, although none are directly known to date. Although diverse forkhead box transcription factors exhibit highly

conserved central DNA binding forkhead domains, they have very different flanking and transactivation sequences (Lam et al., 2013). ENCODE RNA sequencing data demonstrate that a number of forkhead factors are expressed in normal human CD14<sup>+</sup> monocytes, including *FOXJ3*, *FOXP1*, *FOXN3*, *FOXO1*, and *FOXO3*. An alternative possibility is that FOXC1 directly represses through localized binding expression of one or more key transcriptional regulators of monocytic differentiation. For example, expression of *Egr1*, *Klf4*, and *Mef2c* is significantly suppressed in *Hoxa9/FOXC1* AML cells, and all these genes code for critical positive regulators of monocyte differentiation (Laslo et al., 2006; Feinberg et al., 2007; Schüller et al., 2008). Our functional analyses demonstrate that FOXC1 represses expression of *KLF4* and show that restoration of *KLF4* expression in *Hoxa9/FOXC1* AML cells inhibits proliferation and clonogenic potential. Whether FOXC1-mediated gene repression occurs through binding at multiple enhancer or promoter sites across the genome or more specifically through interactions with a master regulator such as PU.1 remains unclear.

The basis for the collaboration of FOXC1 with HOXA9 likewise remains unclear. The somewhat similar immunophenotypes and array expression profiles of murine *Hoxa9/MTV* AMLs versus *Hoxa9/Meis1* AMLs are in keeping with the known function of MEIS1 in stabilizing the interaction of HOXA9 with DNA (i.e., enhancing its potency) (Shen et al., 1997). The fact that *Hoxa9/FOXC1* AMLs appear so different in terms of their immunophenotypes, transcriptomes, and histologies implies that FOXC1 may confer on HOXA9 an alternative activity or perhaps misdirect its binding to distinct enhancer sets. The known activity of forkhead proteins as pioneer transcription factors may be relevant in this regard (Lam et al., 2013).

*FOXC1* occupies a DNA-hypomethylated, DNase-hypersensitive genomic locus in CD34<sup>+</sup> cells that is marked by both H3K4 and H3K27 trimethylation. This suggests the chromatin surrounding this gene is relatively decompacted, and such epigenetic configurations have previously been termed bivalent. Bivalent genes are transcriptionally repressed by Polycomb, and in keeping with this, we were able to induce expression of *FOXC1* in normal human CD34<sup>+</sup> cells by treatment of cells with inhibitors of PRC. The most effective was the dual EZH1/EZH2 inhibitor UNC1999, suggesting EZH1 may compensate for loss of activity of EZH2 when a pure EZH2 inhibitor is used. Nevertheless, the mechanisms underlying loss of Polycomb repression at a single locus in AML require further investigation. Of more than 200 genes with similar chromatin and transcriptional configurations to *FOXC1* in CD34<sup>+</sup> cells, only *HOXB8*, *IRX3*, and *IRX5* were similarly derepressed in a significant proportion of AML cases, indicating that although there is locus-specific loss of Polycomb activity in a substantial proportion of AML cases, there is no generalized failure of suppression of Polycomb marked genes.

Finally, our findings may have therapeutic consequences. For example, in basal-like breast cancer, high *FOXC1* expression renders cells more susceptible to pharmacological inhibition of NF- $\kappa$ B (Wang et al., 2012). Further studies may uncover specific therapeutic targets or approaches in this frequent sub-group of human AML.

## EXPERIMENTAL PROCEDURES

### Human Tissue and Ethical Approval

Use of human tissue was in compliance with the ethical and legal framework of the United Kingdom's Human Tissue Act of 2004. Normal CD34<sup>+</sup> HSPCs surplus to requirements were from patients undergoing autologous transplantation for lymphoma or myeloma. Cells were mobilized using chemotherapy and granulocyte-colony stimulating factor as described (Lee et al., 2005). Their use was authorized by the Salford and Trafford Research Ethics Committee and, for samples collected since 2006, following the written informed consent of donors. Normal human BM was collected with informed consent from healthy adult male donors, with the ethical approval of the Yorkshire Independent Research Ethics Committee. Primary human AML samples were from Manchester Cancer Research Centre's Tissue Biobank (instituted with approval of the South Manchester Research Ethics Committee). Their use was authorized following ethical review by the Tissue Biobank's scientific sub-committee, and with the informed consent of donors.

### Murine Transplantation Experiments

Experiments using mice were approved by the Cancer Research UK Manchester Institute's Animal Ethics Committee and performed under a project license issued by the United Kingdom Home Office, in keeping with the Home Office Animal Scientific Procedures Act of 1986. C57BL/6 (CD45.2<sup>+</sup>) mice were purchased from Harlan. B6.SJL-*Ptprc*<sup>a</sup> *Pepc*<sup>b</sup>/BoyJ (CD45.1<sup>+</sup>) mice were purchased from Jackson Laboratories and bred in house. Further details may be found in [Supplemental Experimental Procedures](#).

### Cell Culture, Reagents, Plasmids, Virus Manufacture, and Flow Cytometry

Details may be found in [Supplemental Experimental Procedures](#).

### Statistical Analyses

Statistical analyses were performed using StatsDirect software version 1.9.7 (StatsDirect), Microsoft Excel, or SPSS for Mac version 22 (IBM).

### RNA Isolation, Quantitative PCR, Exon Arrays, and Bioinformatics Analyses

RNA was extracted using QIAshredder spin columns and an RNeasy Plus Micro kit (Qiagen). Details of protocols used for quantitative PCR, exon arrays, and bioinformatics analyses are in [Supplemental Experimental Procedures](#).

### ACCESSION NUMBERS

Exon array data files from this study are available at the Gene Expression Omnibus (GEO: GSE66256).

### SUPPLEMENTAL INFORMATION

Supplemental Information includes Supplemental Experimental Procedures, seven figures, and nine tables and can be found with this article online at <http://dx.doi.org/10.1016/j.ccell.2015.07.017>.

### AUTHOR CONTRIBUTIONS

T.D.D.S. performed experiments. D.H.W., G.J.S., X.H., J.T.L., and E.L.W. assisted with experiments and data analysis. H.S.L. performed bioinformatics analyses. E.C. performed histopathological analyses. T.D.D.S. and T.C.P.S. designed experiments, analyzed data, and wrote the manuscript. All authors read and approved the final version of the manuscript.

### ACKNOWLEDGMENTS

We thank John Weightman, Jeff Barry, Abi Johnson, and staff members from the Biological Resources Unit for technical assistance; Yaoyong Li for assistance with exon array data processing; Ruud Delwel for sharing the survival data from the Dutch AML cohort; Jane Sowden for the *FOXC1* cDNA; Georges Lacaud for the *KLF4* cDNA; and Chris Womack and staff members at the Clinical Pharmacology Unit at AstraZeneca for access to normal subjects for BM

collection. Analysis of intergenic mutations surrounding *FOXC1* in human AML was carried out using data generated by The Cancer Genome Atlas Research Network as part of dbGAP authorized project 8623, with accession number phs000178.v9.p8. This work was supported by Cancer Research UK grant number C5759/A02901. D.H.W. was supported by a Leukaemia and Lymphoma Research clinical training fellowship.

Received: February 19, 2015

Revised: June 1, 2015

Accepted: July 30, 2015

Published: September 14, 2015

## REFERENCES

- Bloushtain-Qimron, N., Yao, J., Snyder, E.L., Shipitsin, M., Campbell, L.L., Mani, S.A., Hu, M., Chen, H., Ustyansky, V., Antosiewicz, J.E., et al. (2008). Cell type-specific DNA methylation patterns in the human breast. *Proc. Natl. Acad. Sci. U S A* *105*, 14076–14081.
- Cancer Genome Atlas Research Network (2013). Genomic and epigenomic landscapes of adult de novo acute myeloid leukemia. *N. Engl. J. Med.* *368*, 2059–2074.
- Cerami, E., Gao, J., Dogrusoz, U., Gross, B.E., Sumer, S.O., Aksoy, B.A., Jacobsen, A., Byrne, C.J., Heuer, M.L., Larsson, E., et al. (2012). The cBio cancer genomics portal: an open platform for exploring multidimensional cancer genomics data. *Cancer Discov.* *2*, 401–404.
- Feinberg, M.W., Wara, A.K., Cao, Z., Lebedeva, M.A., Rosenbauer, F., Iwasaki, H., Hirai, H., Katz, J.P., Haspel, R.L., Gray, S., et al. (2007). The Kruppel-like factor KLF4 is a critical regulator of monocyte differentiation. *EMBO J.* *26*, 4138–4148.
- Gibbs, K.D., Jr., Jager, A., Crespo, O., Goltsev, Y., Trejo, A., Richard, C.E., and Nolan, G.P. (2012). Decoupling of tumor-initiating activity from stable immunophenotype in HoxA9-Meis1-driven AML. *Cell Stem Cell* *10*, 210–217.
- Goardon, N., Marchi, E., Atzberger, A., Quek, L., Schuh, A., Soneji, S., Woll, P., Mead, A., Alford, K.A., Rout, R., et al. (2011). Coexistence of LMPP-like and GMP-like leukemia stem cells in acute myeloid leukemia. *Cancer Cell* *19*, 138–152.
- Huang, X., Spencer, G.J., Lynch, J.T., Ciceri, F., Somerville, T.D., and Somervaille, T.C. (2014). Enhancers of Polycomb EPC1 and EPC2 sustain the oncogenic potential of MLL leukemia stem cells. *Leukemia* *28*, 1081–1091.
- Ismail, I.H., McDonald, D., Strickfaden, H., Xu, Z., and Hendzel, M.J. (2013). A small molecule inhibitor of polycomb repressive complex 1 inhibits ubiquitin signaling at DNA double-strand breaks. *J. Biol. Chem.* *288*, 26944–26954.
- Kharas, M.G., Yusuf, I., Scarfone, V.M., Yang, V.W., Segre, J.A., Huettner, C.S., and Fruman, D.A. (2007). KLF4 suppresses transformation of pre-B cells by *ABL* oncogenes. *Blood* *109*, 747–755.
- Kikushige, Y., Shima, T., Takayanagi, S., Urata, S., Miyamoto, T., Iwasaki, H., Takenaka, K., Teshima, T., Tanaka, T., Inagaki, Y., and Akashi, K. (2010). TIM-3 is a promising target to selectively kill acute myeloid leukemia stem cells. *Cell Stem Cell* *7*, 708–717.
- Konze, K.D., Ma, A., Li, F., Barsyte-Lovejoy, D., Parton, T., Macnevin, C.J., Liu, F., Gao, C., Huang, X.P., Kuznetsova, E., et al. (2013). An orally bioavailable chemical probe of the Lysine Methyltransferases EZH2 and EZH1. *ACS Chem. Biol.* *8*, 1324–1334.
- Kroon, E., Kros, J., Thorsteinsdottir, U., Baban, S., Buchberg, A.M., and Sauvageau, G. (1998). Hoxa9 transforms primary bone marrow cells through specific collaboration with Meis1a but not Pbx1b. *EMBO J.* *17*, 3714–3725.
- Kume, T., Deng, K.Y., Winfrey, V., Gould, D.B., Walter, M.A., and Hogan, B.L. (1998). The forkhead/winged helix gene Mf1 is disrupted in the pleiotropic mouse mutation congenital hydrocephalus. *Cell* *93*, 985–996.
- Lam, E.W., Brosens, J.J., Gomes, A.R., and Koo, C.Y. (2013). Forkhead box proteins: tuning forks for transcriptional harmony. *Nat. Rev. Cancer* *13*, 482–495.
- Laslo, P., Spooner, C.J., Warmflash, A., Lancki, D.W., Lee, H.J., Sciammas, R., Gantner, B.N., Dinner, A.R., and Singh, H. (2006). Multilineage transcriptional priming and determination of alternate hematopoietic cell fates. *Cell* *126*, 755–766.
- Lee, J.L., Kim, S., Kim, S.W., Kim, E.K., Kim, S.B., Kang, Y.K., Lee, J., Kim, M.W., Park, C.J., Chi, H.S., et al. (2005). ESHAP plus G-CSF as an effective peripheral blood progenitor cell mobilization regimen in pretreated non-Hodgkin's lymphoma: comparison with high-dose cyclophosphamide plus G-CSF. *Bone Marrow Transplant.* *35*, 449–454.
- Mansour, M.R., Abraham, B.J., Anders, L., Berezovskaya, A., Gutierrez, A., Durbin, A.D., Etchin, J., Lawton, L., Sallan, S.E., Silverman, L.B., et al. (2014). Oncogene regulation. An oncogenic super-enhancer formed through somatic mutation of a noncoding intergenic element. *Science* *346*, 1373–1377.
- Nishimura, D.Y., Swiderski, R.E., Alward, W.L., Searby, C.C., Patil, S.R., Bennet, S.R., Kanis, A.B., Gastier, J.M., Stone, E.M., and Sheffield, V.C. (1998). The forkhead transcription factor gene FKHL7 is responsible for glaucoma phenotypes which map to 6p25. *Nat. Genet.* *19*, 140–147.
- Omatsu, Y., Seike, M., Sugiyama, T., Kume, T., and Nagasawa, T. (2014). Foxc1 is a critical regulator of hematopoietic stem/progenitor cell niche formation. *Nature* *508*, 536–540.
- Ray, P.S., Wang, J., Qu, Y., Sim, M.S., Shamonki, J., Bagaria, S.P., Ye, X., Liu, B., Elashoff, D., Hoon, D.S., et al. (2010). FOXC1 is a potential prognostic biomarker with functional significance in basal-like breast cancer. *Cancer Res.* *70*, 3870–3876.
- Saito, Y., Kitamura, H., Hijikata, A., Tomizawa-Murasawa, M., Tanaka, S., Takagi, S., Uchida, N., Suzuki, N., Sone, A., Najima, Y., et al. (2010). Identification of therapeutic targets for quiescent, chemotherapy-resistant human leukemia stem cells. *Sci. Transl. Med.* *2*, 17ra9.
- Schüler, A., Schwieger, M., Engelmann, A., Weber, K., Horn, S., Müller, U., Arnold, M.A., Olson, E.N., and Stocking, C. (2008). The MADS transcription factor Mef2c is a pivotal modulator of myeloid cell fate. *Blood* *111*, 4532–4541.
- Shen, W.F., Montgomery, J.C., Rozenfeld, S., Moskow, J.J., Lawrence, H.J., Buchberg, A.M., and Largman, C. (1997). AbdB-like Hox proteins stabilize DNA binding by the Meis1 homeodomain proteins. *Mol. Cell. Biol.* *17*, 6448–6458.
- Thorsteinsdottir, U., Mamo, A., Kroon, E., Jerome, L., Bijl, J., Lawrence, H.J., Humphries, K., and Sauvageau, G. (2002). Overexpression of the myeloid leukemia-associated Hoxa9 gene in bone marrow cells induces stem cell expansion. *Blood* *99*, 121–129.
- Vaquerez, J.M., Kummerfeld, S.K., Teichmann, S.A., and Luscombe, N.M. (2009). A census of human transcription factors: function, expression and evolution. *Nat. Rev. Genet.* *10*, 252–263.
- Verma, S.K., Tian, X., LaFrance, L.V., Duquenne, C., Suarez, D.P., Newlander, K.A., Romeril, S.P., Burgess, J.L., Grant, S.W., Brackley, J.A., et al. (2012). Identification of Potent, Selective, Cell-Active Inhibitors of the Histone Lysine Methyltransferase EZH2. *ACS Med. Chem. Lett.* *3*, 1091–1096.
- Wang, J., Ray, P.S., Sim, M.S., Zhou, X.Z., Lu, K.P., Lee, A.V., Lin, X., Bagaria, S.P., Giuliano, A.E., and Cui, X. (2012). FOXC1 regulates the functions of human basal-like breast cancer cells by activating NF- $\kappa$ B signaling. *Oncogene* *31*, 4798–4802.
- Wiseman, D.H., Greystoke, B.F., and Somervaille, T.C. (2014). The variety of leukemic stem cells in myeloid malignancy. *Oncogene* *33*, 3091–3098.
- Wouters, B.J., Löwenberg, B., Erpelinck-Verschueren, C.A., van Putten, W.L., Valk, P.J., and Delwel, R. (2009). Double CEBPA mutations, but not single CEBPA mutations, define a subgroup of acute myeloid leukemia with a distinctive gene expression profile that is uniquely associated with a favorable outcome. *Blood* *113*, 3088–3091.
- Xia, L., Huang, W., Tian, D., Zhu, H., Qi, X., Chen, Z., Zhang, Y., Hu, H., Fan, D., Nie, Y., and Wu, K. (2013). Overexpression of forkhead box C1 promotes tumor metastasis and indicates poor prognosis in hepatocellular carcinoma. *Hepatology* *57*, 610–624.
- Yu, M., Bardia, A., Wittner, B.S., Stott, S.L., Smas, M.E., Ting, D.T., Isakoff, S.J., Ciciliano, J.C., Wells, M.N., Shah, A.M., et al. (2013). Circulating breast tumor cells exhibit dynamic changes in epithelial and mesenchymal composition. *Science* *339*, 580–584.
- Zhou, X., Maricque, B., Xie, M., Li, D., Sundaram, V., Martin, E.A., Koebbe, B.C., Nielsen, C., Hirst, M., Farnham, P., et al. (2011). The Human Epigenome Browser at Washington University. *Nat. Methods* *8*, 989–990.